BMC Gastroenterology

RESEARCH Open Access

Efficacy of B - mode and elastography ultrasound technique in the prediction of *Helicobacter pylori*: a prospective study

Abdulaziz Hussein[1,2], Awadia Gareeballah[3*], Amin Mohsen Amer[4], Sultan Abdulwadoud Alshoabi[3], Moawia Gameraddin[3], Maisa Elzaki[3], Walaa Alsharif[3], Fahad H. Alhazmi[3], Raga Ahmed Abouraida[5], Kamal Alsultan[3], Fathelrehman Ahmed Elajab[3] and Mohamed Adam[5]

Abstract

Background *Helicobacter pylori* (HP) affect nearly 50% of the world's population and can colonize the submucosal and mucosal layers of the stomach wall, causing inflammation leading to a thickening of these layers. The study aimed to evaluate the application value of transabdominal ultrasonography combined with elastography in the prediction of HP using HP Fecal Antigen Test as gold standard.

Method This prospective case-control study was conducted in 174 participants classified into three groups: **Group A**: Symptomatic patients with thickened stomach antral and evident HP infection on fecal antigen test results, **Group B**: Symptomatic patients with thickened antral and no evident HP infection on fecal antigen test results, and **Group C**: control group of asymptomatic individuals with negative HP screening to predict the diagnostic accuracy of B-mode ultrasound and elastography in the prediction of HP pylori.

Results Positive HP patients had higher values of antral wall thickness (AWT), mucosal layer thickness (MLT), MLT/AWT ratio, SR (strain ratio), and a combination of AWT and SR: 5.57 ± 0.55 mm, 2.96 ± 0.45 mm, 0.53 ± 0.06 mm, 3.21 ± 0.43, and 8.79 ± 0.68 mm, respectively. In comparison, negative HP patients had values of 4.61 ± 0.47 mm, 2.05 ± 0.42 mm, 0.41 ± 0.08 mm, 2.51 ± 0.42 mm, and 7.13 ± 0.62 mm, respectively, and the control groups had values of 3.53 ± 0.36 mm, 1.47 ± 0.25 mm, 0.40 ± 0.06 mm, 1.81 ± 0.41, and 5.35 ± 0.55 mm, respectively ($p < 0.001$). The sensitivity of B-mode ultrasonography, elastography, and the combination of the two was 98%, 95.1%, and 98.4%, respectively, and the diagnostic accuracy was 98.4%, 98.3%, and 100%, respectively.

Conclusion B-mode ultrasonography and elastography exhibit high discriminatory power in distinguishing symptomatic HP patients from normal individuals and differentiating + HP from - HP, with greater discriminatory power when combined both modes.

Keywords B-mode ultrasonography, Elastography, *Helicobacter pylori* gastritis, Antral wall thickness, Mucosal layer thickness, Strain ratio (SR)

*Correspondence:
Awadia Gareeballah
awadhia1978@gmail.com

Full list of author information is available at the end of the article

Introduction

In 2007, the American College of Gastroenterology clinical guidelines noted that *Helicobacter pylori* (HP) is one of the most common chronic bacterial infections in humans [1], affecting nearly 50% of the world's population. It can colonize the submucosal and mucosal layers of the stomach wall, causing inflammation and erosion, leading to a thickening of these layers in patients with HP gastritis, peptic ulcer diseases, and mucosa-associated lymphoid tissue lymphoma [2, 3]. According to the World Health Organization, HP infection contributes to 75% of gastric cancers [4].

HP gastric infection can be diagnosed using invasive and non-invasive diagnostic methods, each of which has advantages and disadvantages. The North American Society of Pediatric Gastroenterology, Hepatology, and Nutrition and the European Society for Pediatric Gastroenterology, Hepatology, and Nutrition recommend biopsy-based testing based on a positive culture or histopathology for the initial diagnosis of HP gastritis [2, 5]. Image-enhanced endoscopy plays a significant role in detecting gastritis and early gastric cancer. Linked color imaging is useful for diagnosing and evaluating gastritis, gastric metaplasia, and some precancerous lesions [6]. However, endoscopy is an invasive, expensive sedation-based procedure, making it impractical for diagnosing HP gastritis.

The antrum of stomach is typically the predominant location of inflammation, with the submucosal layer often being inhabited by HP. Radiologically, thickening of the gastric wall is a significant indicator of gastrointestinal diseases. The thickening of the mucosal layer is believed to be caused by erosion due to HP proliferation, resulting in an increase in thickness. Likewise, the submucosal layer, along with the mucosal layer and muscularis mucosa, may also thicken in accordance with the level and seriousness of inflammatory alterations [7]. Transabdominal ultrasonography is an effective imaging modality for visualizing and measuring the thickness of gastric wall layers. It is a useful imaging modality for predicting HP gastritis by measuring the thickness of the gastric antral walls and mucosal layers [8]. However, ultrasonography is an operator-dependent modality, with artifacts in the gastrointestinal tract having a false negative effect on diagnosis [9]. Ultrasonography also has inherent limitations in its sensitivity and depth of penetration, which may impact its accuracy [10].

Elastography is a method that has been developed to assess the mechanical properties of tissues non-invasively, specifically focusing on their stiffness. There are various elastography technologies currently available. Strain elastography allows for the quantitative imaging of strain and elastic modulus distributions in soft tissues: by applying tissue compression, the strain profile along the transducer axis is calculated and then converted into an elastic modulus profile based on the measurement of the stress applied. Typically, strain imaging or ultrasound elasticity imaging (UEI) refers to the technique where tissue deformation is induced by pressing on the tissue with an ultrasound transducer (external force) and then recorded simultaneously with real-time US images. Various techniques involving a combination of static or dynamic deformations to internal or external forces have been explored, ending with the current use of strain elastography - with pressure being applied manually or through cardiovascular pulsation - in various fields of clinical medicine, such as characterizing breast lesions [11]. The concept that normal and pathologic tissues possess distinct mechanical properties, primarily attributed to the modified equilibrium of normal, fibrotic, and/or inflammatory tissue components, is supported by the widespread implementation of elastography in diverse clinical scenarios [11]. Inflammation and erosion resulting from H. pylori infection have the potential to modify the elasticity of the gastric wall [2].

The significant limitations of the currently available imaging methods for HP gastritis diagnosis create the need for more obvious non-invasive imaging methods to diagnose. Utilization of transabdominal ultrasound elastography for analyzing the gastric wall thickness and stiffness alterations could offer valuable clinical advantages in diagnosis of HP, this study assessed the diagnostic performance of B-mode ultrasonography based on gastric wall thickening and strain elastography stiffness alteration based on strain ratio (SR) in diagnosing of HP using a non-invasive rapid HP Fecal Antigen Test as gold standard to confirm the presence of HP, to the best of our knowledge, this study is the first to explore this method in Yemen.

Materials and methods

This prospective case-control designed study was conducted to predict the diagnostic accuracy of B-mode ultrasound and elastography in diagnosing positive HP pylori based on noninvasive fecal antigen test results for detection of H pylori as reference standard, from November 2023 to January 2024. The data were collected from the Dr. Ahmed Alzomor Specialized Polyclinic (IBB City, Yemen). A total of 174 participants were randomly selected and classified into three groups: **Group A**: Symptomatic patients with thickened antral and evident HP infection on fecal antigen test results (61 patients), **Group B**: Symptomatic patients with thickened antral and no evident HP infection on fecal antigen test results (54 patients), and **Group C**: control group of asymptomatic individuals with negative HP screening (59 participants).

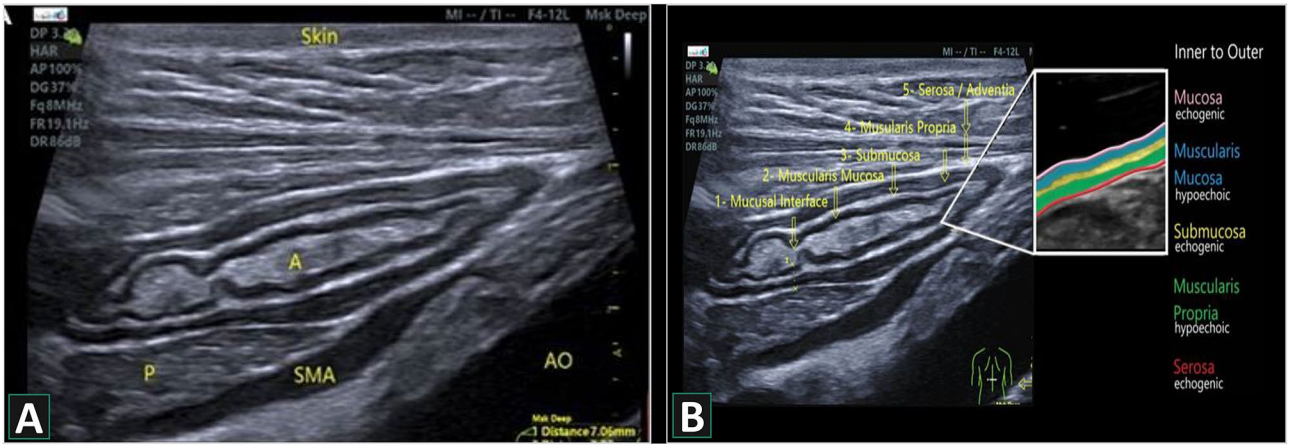

Fig. 1 (**A**): Sonographic image shows Epigastric – antrum at sagittal plane illustrating the anatomic landmarks for identify antrum at epigastrium. A = antrum; L = liver; P = pancreas; SMA = superior mesenteric artery; AO = aorta. (**B**): Trans abdominal sonography (B – mode) illustrate the normal gut stratification of bowel layers (antral area); R.t = Right; L.t = Left

Inclusion criteria

Only adult participants (≥18 years) were included in this study. Patients from Groups A and B were selected from symptomatic individuals suspected of having HP infection and attended a laboratory unit for elective diagnostic tests of HP (stool antigen assay). They were then allocated to either Groups A or B, according to their HP infection status (Group A with +HP and Group B with –HP). Participants who were smokers and Qat leaf chewers were included, as both were risk factors.

Exclusion criteria

1. Patients with previously known diseases thought to affect the intestinal wall (celiac disease and inflammatory bowel disease) and hepatitis.
2. Patients with a history of hepatic congestive gastropathy, gastric cancer, melanomas, varices, gastric surgery, radiotherapy, coagulopathy, alcohol intake, Crohn's disease, end-organ failure, immunocompromised, acute pancreatitis, any cause of anasarca, peptic ulcer disease, HP eradication, GIT bleeding, the use of non-steroidal anti-inflammatory drugs, and acid-suppressing drugs or antibiotics used within one month.
3. Patients with conditions that could lead to gut wall thickening, such as severe edema or ascites, gastric wall varices or mass, and infiltrative diseases.

Study variables

The study variables included demographic characteristics (age, gender, residence, weight, and body mass index (BMI), risk factors (smoking and Qat chewing), clinical presentations (e.g., gastric pain, vomiting, and nausea), and the results of HP lab tests (+Ve/-Ve). Other variables are the measurements of antral wall thickness (AWT), mucosal wall thickness (MLT), (MLT/AWT ratio), and strain elastography ratio in all the study groups.

B- mode and elastography ultrasound techniques

Equipment and preparation

Two ultrasound machines were used for the examination: VINNO E35 (4–16 MHz, China, serial number U0312JJ008) and Samsung HS30 (4–12 MHz, Korea, serial number HS3NN3C/GB). A linear array high-frequency transducer was used (4–16 and 4–12 MHz). All gastric examinations were performed after four hours of fasting. All patients drank 500–800 ml of plain water and wait about 10–15 min to allow the air bubbles to move away. Blinded to clinical presentation and laboratory results, both B-mode and elastography ultrasound technique performed by sonographic specialist with experience in US-EG examination, then two experienced radiologists specialized in US-EG procedures, conducted a comprehensive review of all measurements, ensuring that only high-quality strain measurement were recorded for further analysis.

Conventional B-mode transabdominal ultrasound scan and measurements

A gastric scan was performed with the patients in a supine position and the right lateral decubitus (RLD), the scan is started by positioning the transducer in the sagittal plane in the epigastrium region immediately below xiphisternum. The transducer was then swept from the left to the right subcostal margins, seeking the landmarks (Aorta, SMA, head and neck of pancreas) until the gastric antrum was identified in short axis, The liver used as an acoustic window to visualize the gastric antrum, which can be distinguished from other hollow viscera such as duodenum or bowel by its thick, hypoechoic muscularis

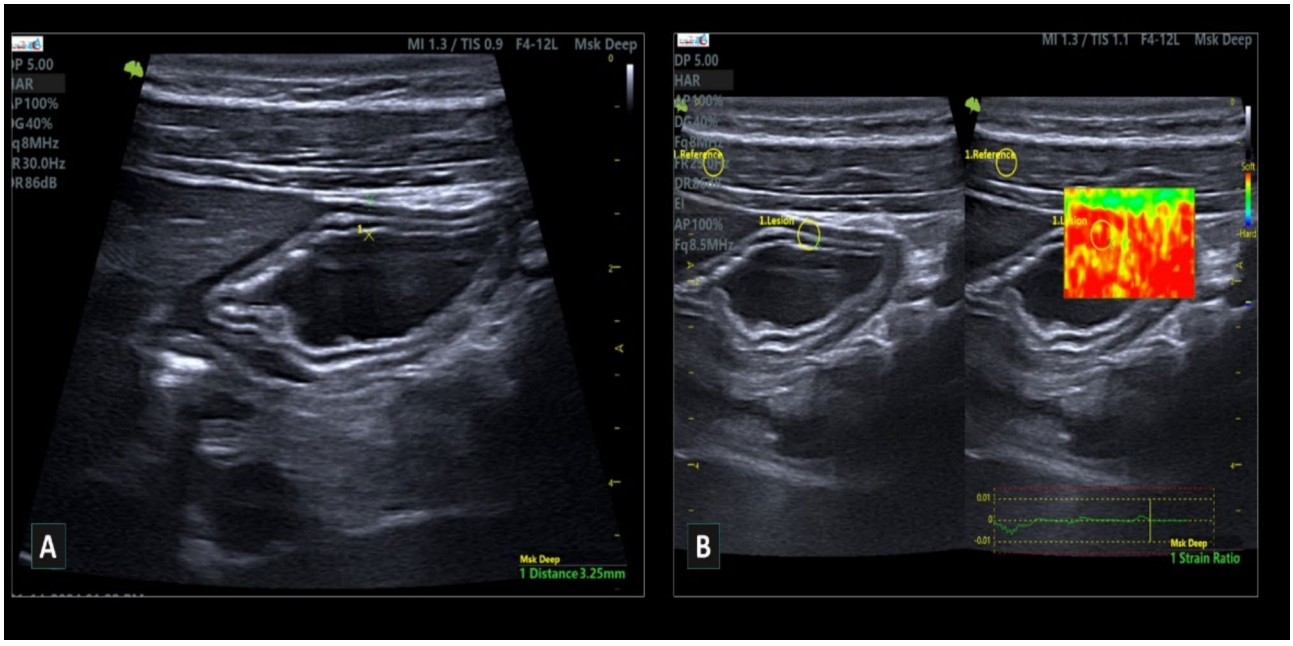

Fig. 2 (**A**): B-mode sonogram for calculating anterior gastric wall (antral wall thickness [AWT] = 3.25 mm) and (**B**): Elastogram in color coding for which the inner circle region of interest (ROI) in the colored box (Lesion) represents the antral gastric wall electrographic value, and the outer circle (Reference) represents the normal neighboring structure. The strain elastography ratio was automatically calculated using a device that divided the strain value of the inner box of the antral wall by the strain value of the normal surrounding structure

layer along with the hyperechoic serosa and mucosal layers, the transducer is sliding from left to right, or right to left, and heel-to-toe maneuvers or transducer rotation to clearly demonstrate the antrum in short axis at the level of the aorta, and to minimalize obliquity in antral views. After a clear visualization of the gastric wall as a five-layered structure, Fig. 1. Then, the gastric wall thickness was measured at the cross-section of the antrum, especially the anterior antral wall, with a longitudinal section of the superior mesenteric artery as a landmark. Both muscular layers (interna/superficial mucosa and the externa mucosa) were focused and measured, by calculate the measurement three time and get an average. Figure (2-a).

Elastography strain ratio calculation methods

Five strain measurements were obtained from the stomach wall via a subxiphoid approach during suspended respiration. A 2×2 cm strain color map (elastogram) and a 0.5 cm were placed manually around the region of interest (ROI). The ROI was placed in areas of optimal color fill. The depth of measurement was automatically calculated using an ultrasound device, as shown in Fig. 2-B.

HP fecal antigen test

In this study, the one-step HP antigen (Ag) test involved collecting a stool sample from the patient and preparing it by mixing it with a sample extraction buffer b). The prepared sample was then added to the sample well of a test cassette. After a specified waiting period, the test results were interpreted by observing the appearance of colored lines in the control region (C) and the test region (T) of the cassette. A colored line in the control region (C) confirms the validity of the test, while a line in the test region (T) indicates the presence of the HP antigen, suggesting a positive result for HP infection. The absence of a line in the test region (T) denotes a negative result, the test kits used, and procedure shown in Fig. 3 below.

Statistical analysis

The data was analyzed using SPSS 27 for Windows (SPSS Inc., Chicago, IL, USA) & HP for windows (Software, Palo Alto, America). Descriptive statistics such as percentages and frequency distribution were used to describe the qualitative variables, mean and standard deviation were used for quantitative variables. Chi-square test was used to assess the correlation between categorical variables, Cohen's weighted Kappa test was used to assess the agreement of both ultrasound methods in the prediction of HP, moreover, to evaluate the diagnostic performance of B-mode, elastography and combined B- mode and elastography in the prediction of HP, ROC (Receiver Operating Characteristic) curve analysis was used to estimate sensitivity, specificity, accuracy, and AUC (area under the curve), all tests were two-sided, with p-value <0.05 and <0.01 considered statistically significance.

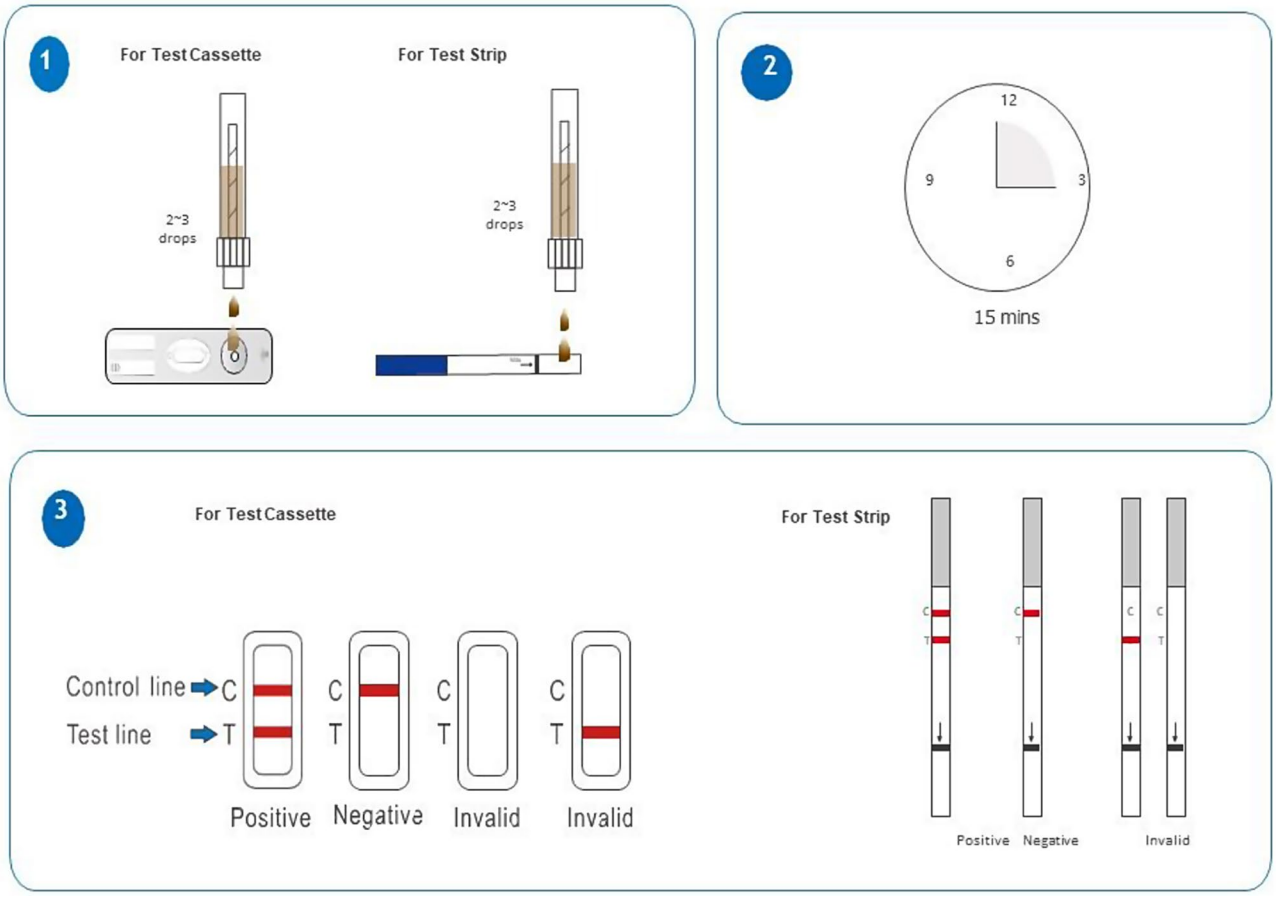

Fig. 3 Shows H. pylori test procedure (product of Wondfo One Step H. Pylori Feces Test) used in this study and the examination

Results

The results indicated no statistically significant differences in age, gender, residence, and BMI among the study groups ($p>0.05$). (Table 1).

This study showed that the risk factors in Group A—Qat chewing, smoking, and a family history or infection history of HP—were distributed as follows: 54%, 26%, 20%, and 23%, respectively. (Fig. 4)

The symptoms evaluated in this study included gastric pain (stomachache), nausea, vomiting, loss of appetite, abdominal bloating and distention, and headaches. The results indicated that gastric pain, loss of appetite, and nausea or vomiting were the most common clinical presentations in Group A (50, 59.9%; 28, 66.7%; 18, 64.3%; and 18, 66.7%, respectively), while gastric pain and abdominal bloating and distention were common among Group B (34, 40.5% and 23, 62.2%) (Table 2).

The results showed statistically significant differences among the three groups for all parameters ($p<0.001$). The findings indicate that the positive HP patients had higher values of AWT, MLT, MLT/AWT ratio, SR, and ES–UG (5.57±0.55 mm, 2.96±0.45 mm, 0.53±0.06 mm, 3.21±0.43, and 8.79±0.68, respectively) than the negative non-HP group (4.61±0.47 mm, 2.05±0.42 mm, 0.41±0.08 mm, 2.51±0.42 mm, and 7.13±0.62 mm, respectively) and the control group (3.53±0.36 mm, 1.47±0.25 mm, 0.40±0.06 mm, 1.81±0.41 mm, and 5.35±0.55 mm, respectively).(Table 3).

For predicting symptomatic HP from normal subject groups, the results indicated good diagnostic accuracy for B-mode sonography and elastography. They showed good discriminatory power in distinguishing symptomatic HP patients from normal subjective groups. The statistical significance of the results was assessed using p-values, and all comparisons were significant ($p<0.001$), indicating the reliability of the observed differences (Table 4; Fig. 5).

The results showed moderate to good diagnostic accuracy for both B-mode sonography and elastography for differentiating HP+from non-HP. The sensitivity values ranged from 76 to 91% for B-mode sonography measurements (AWT) and from 58.9 to 81.4% for elastography (SR). The specificity values were in the range of 73.3–93.3% for B-mode sonography (AWT) and 65.81–89.12% for elastography. The accuracy values ranged from 84.4 to 99.0% for B-mode sonography (AWT) and from 83.2

Table 1 Demographic characteristics of the study group

Variables	Demographic characteristic's			*P*-value
Age	Study Groups	Mean ± SD	Median (Range)	
	Group – A (H.p +)	34.54 ± 12.90	33 (18–62)	0.321
	Group - B (H.p -)	36.11 ± 13.90	36.11 (18–70)	
	Group – C (Control)	38.53 ± 16.41	38.53 (18–78)	
	Total	36.38 ± 14.51	33 (18–78)	
BMI	Group – A (H.p +)	25.01 ± 5.08	23.5 (17.6–35)	0.969
	Group - B (H.p -)	24.90 ± 4.49	23.5 (17.9–34.4)	
	Group – C (Control)	25.19 ± 4.47	24.4 (18.5–34.6)	
	Total (kg/m2)	25.06 ± 4.67	23.3 (17.6–35)	
Gender	Study Groups	Frequency and %		0.393
		Male	Females	
	Group – A (H.p +)	25 (41.0%)	36 (59.0%)	
	Group - B (H.p -)	23 (42.6%)	31 (57.4%)	
	Group – C (Control)	31 (52.5%)	28 (47.5%)	
	Total	(79; 45.4%)	(95; 54.6%)	
Residence	Study groups	Frequency and %		0.941
		Rural	Urban	
	Group – A (H.p +)	35 (57.4%)	26 (42.6%)	
	Group – B (H.p -)	30 (55.6%)	24 (44.4%)	
	Group – C (Control)	32 (54.2%)	27 (45.8%)	
	Total (N; 100%)	97 (55.7%)	77 (44.3%)	

to 93.5% for elastography (SR). The AUROC values were 0.97 for B-mode sonography (AWT) and 0.80 for elastography (SR), indicating good diagnostic accuracy. These findings suggest that both B-mode sonography and elastography can be useful for distinguishing HP + from non-HP. The statistical significance of the results was assessed using p-values, and all comparisons were found to be significant ($p < 0.001$), indicating the reliability of the observed differences (Table 5; Fig. 6).

Table 2 Distribution of the study sample according to the manifested symptoms

Symptoms	Group – A (H.*p* +)		Group - B (H.*p* -)		*P*-value
	Yes	No	Yes	No	
Gastric pain (Stomachache)	50 (59.9%)	11(35.5%)	34(40.5%)	20 (64.5%)	0.022
Nausea	18 (64.3%)	43 (49.4%)	10 (35.7%)	44 (50.6%)	0.171
Vomiting	18 (66.7%)	43 (48.9%)	9 (33.3%)	45 (51.1%)	0.105
Loss of appetite	28 (66.7%)	33 (45.2%)	14 (33.3%)	40 (54.8%)	0.026
Abdominal bloating/distention	14 (37.8%)	47 (60.3%)	23 (62.2%)	31 (39.7%)	0.024
Headache	5 (35.7%)	56 (55.4%)	9 (64.3%)	45 (44.6%)	0.166

For differentiating symptomatic HP patients from normal subjective groups with optimal cut–off values—AWT (B-mode) < 4.95 mm, strain ratio elastography < 2.85, and US–EG < 7.84—B-mode sonography achieved a good sensitivity rate of 93.4% (81–95%), while elastography achieved 95.1% (80–96.5%). These values were elevated when combined evaluations were used (98.4% [89.4–100%]). Similarly, the accuracy values ranged from 95.83% in B-mode to 99.26% for the combined B-mode and elastography. The PPV and NPV values were also

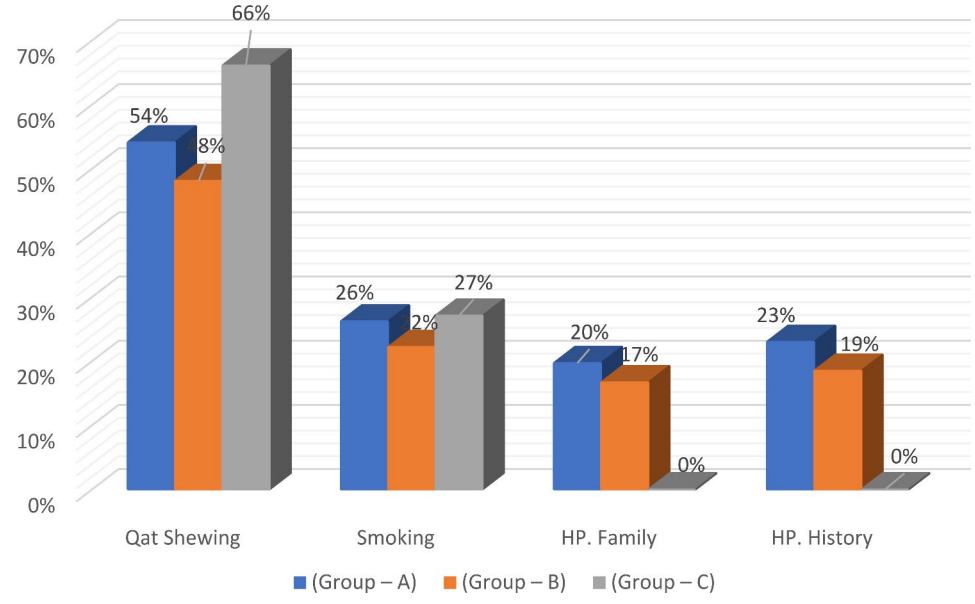

Fig. 4 Distribution of risk factors for HP among the study groups

Table 3 Comparison between study groups regarding ES–US measurements among study groups

Parameters	Groups	Mean±(SD)	Median (range)	95% Confidence Interval for Mean		*P*-value
				Lower bound	Upper bound	
AWT	Positive	5.57 ± 0.55	5.54 (4.96–7)	5.43	5.71	*< 0.001
	Negative	4.61 ± 0.47	4.87 (3.76–6)	4.49	4.75	
	Control	3.53 ± 0.36	3.50 (3–3.9)	3.44	4.1	
MLT	Positive	2.96 ± 0.45	2.87 (2.36–3.98)	2.84	3.08	*< 0.001
	Negative	2.05 ± 0.42	2.18 (1.02–3.20)	1.93	2.16	
	Control	1.47 ± 0.25	1.53 (0.92–1.98)	1.41	1.54	
MLT/AWT Ratio	Positive	0.53 ± 0.06	0.53 (0.41–0.75)	0.51	0.55	*< 0.001
	Negative	0.41 ± 0.08	0.43 (0.21–0.55)	0.39	0.43	
	Control	0.40 ± 0.06	0.40 (0.27–0.58)	0.39	0.42	
SR	Positive	3.21 ± 0.43	3.14 (1.92–4.50)	3.10	3.32	*< 0.001
	Negative	2.51 ± 0.42	2.44 (1.40–3.72)	2.40	2.63	
	Control	1.81 ± 0.41	1.67 (0.50–3.03)	1.71	1.92	
US - EG	Positive	8.79 ± 0.68	8.71 (7.30–10.6)	8.61	8.96	*< 0.001
	Negative	7.13 ± 0.62	7.23 (5.38–8.62)	6.97	7.30	
	Control	5.35 ± 0.55	5.34 (3.87–6.93)	5.20	5.5	

*AWT (antral wall thickness), MLT (mucosal layer thickness), MLT/AWT ratio, SR (strain ratio) and combination of AWT plus SR

Table 4 Diagnostic accuracy of B-mode sonography and elastography for differentiating symptomized HP patients from normal subjective groups (versus control group)

Parameters	SN % (95% CI)	SP (95% CI)	Accuracy % (95% CI)	AURC (95% CI)	*P*-value
AWT	(72.1–93.1%)	(88–99.98%)	(86.16–97.9%)	0.99	*< 0.001
MLT	(75.4–96.7%)	(94.9–100%)	(83.56–99.8%)	1	*< 0.001
MLT/AWT	(78–88%)	(82–90%)	(91.2–98%)	0.93	*< 0.001
SR	(95.3–98.4%)	(83–94%)	(81–95%)	0.98	*< 0.001

*AWT (antral wall thickness), MLT (mucosal layer thickness), MLT/AWT ratio, SR (strain ratio) and combination of AWT plus SR, SN: Sensitivity, SP: specificity. AUROC: Area Under Receiver Operating Characteristic curve, $p<0.05$ is significant

Table 5 Diagnostic accuracy of B-mode sonography and elastography for differentiating symptomized HP patients from non-HP patients (versus non-HP)

Parameters	SN % (95% CI)	SP (95% CI)	Accuracy % (95% CI)	AURC (95% CI)	*P*-value
AWT	(76–91%)	(73.3–93.3%)	(84.41 -99%)	0.97	*< 0.001
MLT	(70–88%)	(74.45–95.6%)	(91.5–99.5%)	0.98	*< 0.001
MLT/AWT	(69.5–87.4%)	(76–89.3%)	(88.2–95%)	0.86	*< 0.001
SR	(58.9–81.4%)	(65.81–89.12%)	(83.2–93.5%)	0.80	*< 0.001

*AWT (antral wall thickness), MLT (mucosal layer thickness), MLT/AWT ratio, SR (strain ratio) and combination of AWT plus SR, SN: Sensitivity, SP: specificity. AUROC: Area Under Receiver Operating Characteristic curve

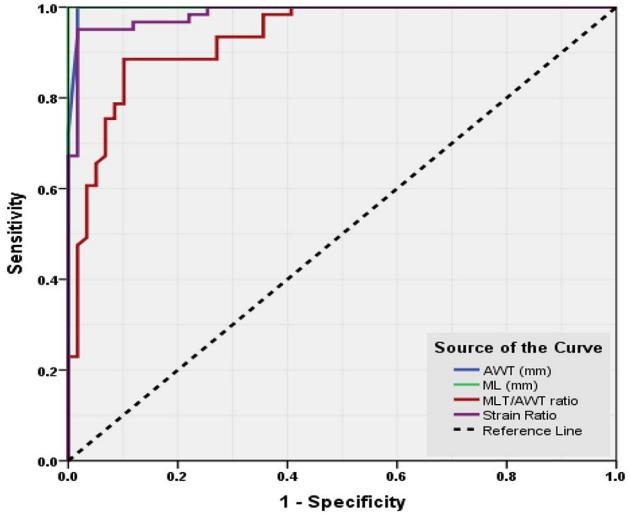

Fig. 5 ROC curve analysis for diagnostic performance of B-mode sonography and elastography for identifying HP-based etiology related to control group

consistently high when both B-mode and elastography were used for HP diagnosis. Kappa statistics, which measure the agreement between the combined evaluation and the actual diagnosis, were also high, ranging from 0.92 to 0.98, reflecting significant agreement. The AUROC curve, which assesses the overall diagnostic accuracy, was excellent, ranging from 0.98 for elastography to 1.00 when B-mode and elastography were combined (Table 6; Fig. 7).

Similarly, the results indicated good diagnostic performance for predicting HP from non-HP at the following optimal cut values: AWT < 4.98 mm, strain ratio elastography < 2.76 and US–EG < 7.58. B-mode sonography achieved a sensitivity of 98% (89.2–100%), and

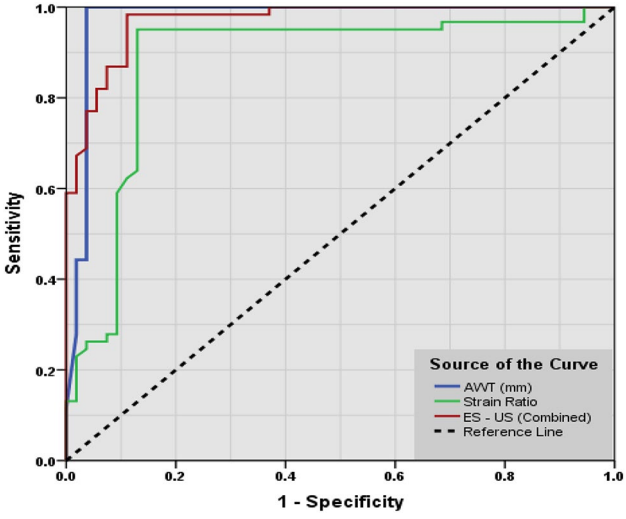

Fig. 6 ROC curve analysis of the diagnostic performance of B-mode sonography and elastography in differentiating HP-based etiology and non-HP group

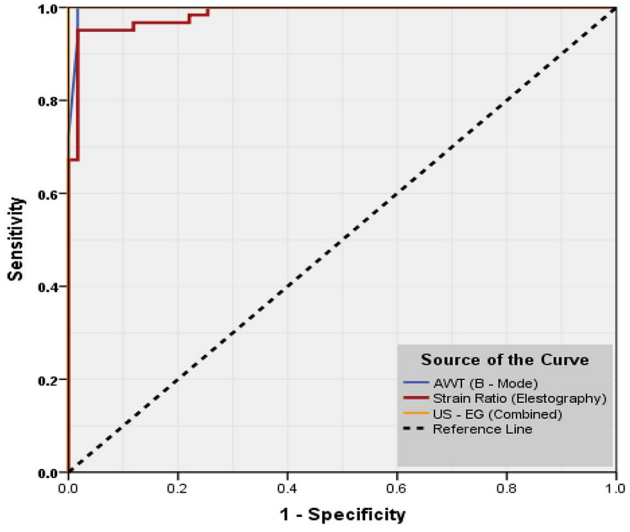

Fig. 7 ROC curve analysis for the diagnostic performance of B-mode sonography, elastography, and combined evaluation for differentiating patients with HP (+) etiologies from the control group

Table 6 Diagnostic performance of B-mode sonography, elastography, and combined evaluation for identifying symptomized HP (+) patients from normal subjective groups (versus control group)

Parameters	B – mode sonography	Elastography	Combined
SN	93.4% (81–95)	95.1% (80–96.5)	98.4% (89.4–100)
SP	98.3% (94–100)	98.3% (92–98.3)	100% (90.55–100)
Accuracy	95.83% (85–96.8)	96.66% (87.43–98.2)	99.26% (89.9–99)
PPV	98.3% (94–99)	98.3% (93.4–100)	100% (91.3–100)
NPV	93.5% (85.4–98.1)	95.1% (88–99.34)	98.3% (89–100)
AUROC	0.99	0.98	100
Kappa	0.92	0.93	0.98
P-value	*< 0.001	*< 0.001	*< 0.001

*(Cut – off values): AWT < 4.95 mm, Strain Ratio – Elastography < 2.85 and US – EG < 7.84.PPV: Positive Predicting values, NPV: Negative Predicting values, SN: Sensitivity, SP: specificity. AUROC: Area Under Receiver Operating Characteristic curve, Kappa: 95% CI: 95% Confidence Interval; $p < 0.05$ is significant

Table 7 Diagnostic performance of elastography, B-mode sonography, and combined evaluation for differentiating HP (+) etiology from that of non-HP gastritis (versus non-HP gastritis)

Parameters	B – mode sonography	Elastography	Combined
SN	98% (89.2–100)	95.1% (88–98.4)	98.4% (91.8–100)
SP	83.3% (79.1–86.7)	85.2% (79.6–88)	88.9% (86.4–91)
Accuracy	92.17% (83–94.3)	90.43% (87–93.7)	98.39% (89–100)
PPV	87.1% (76–91.6)	87.9% (81.3–90)	90% (88.2 -92.08)
NPV	100% (94.2–100)	93.9% (84 -95.2)	98% (91–99.5)
AUROC	0.99	0.98	100
Kappa	0.92	0.93	0.98
P-value	*< 0.001	*< 0.001	*< 0.001

*(Cut – off values): AWT < 4.98 mm, Strain Ratio – Elastography < 2.76 and US – EG < 7.58. SN: Sensitivity, SP: specificity. PPV: positive predictive value, NPV: negative predictive value, AUROC: Area Under Receiver Operating Characteristic curve

elastography achieved 95.1% (88–98.4%). The combined evaluation showed the highest sensitivity, which could reach up to 98.4% (91.8–100%). The specificities ranged from 83.3% using B-mode to 88.9% using combined evaluation, indicating a good ability to correctly predict non-HP patients. The accuracy values were above 90% for the three methods, with PPV and NPV values of 87.1% for B-mode, 90% for the combined method, and 93.9% for elastography. When both B-mode and elastography were combined, the accuracy values were 100% and 98.0%, respectively. The AUROC values were again high, ranging from 0.98 to 1.00, suggesting excellent diagnostic prediction accuracy of HP when B-mode and elastography were combined. The kappa statistics showed a significant agreement between the combined evaluation and the actual diagnosis (0.92 in B-mode and 0.98 when both methods were combined in diagnosis) (Table 7; Fig. 8).

Discussion

Aiming to introduce a non-invasive, more practical imaging method for predicting HP, this study aimed to investigate the utility of the gastric wall in predicting the diagnosis of HP infection thickening using transabdominal ultrasonography and elastography imaging modalities. HP infection in gastric mucosa is the main risk factor for gastric cancer [12], and the discovery of HP has revolutionized our understanding of gastroduodenal disease [13]. HP bacterial infection affects human gastric mucosa and has been found to alter normal gastric physiology, including ghrelin-producing cells that produce ghrelin. Ghrelin is anti-inflammatory and anti-apoptotic, and the loss of ghrelin leads to a loss of appetite and may

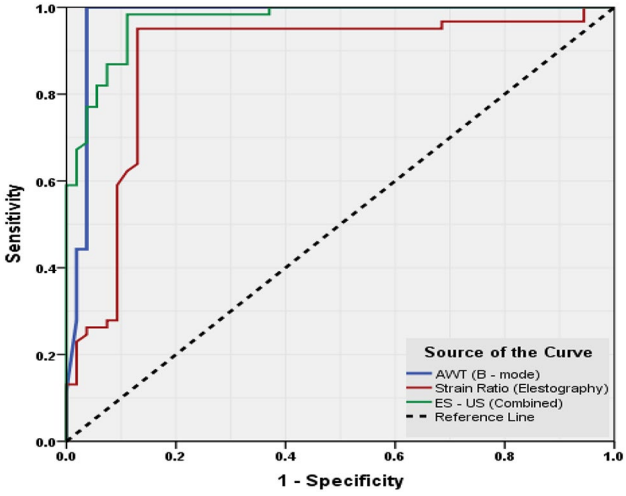

Fig. 8 ROC curve analysis for the diagnostic performance of elastography, B-mode sonography, and combined evaluation for differentiating HP-based etiology from that of non-HP gastritis

impair healing during gastritis [14]. Ghrelin suppression responses have been observed in chronic gastritis and HP infection [15]. The current case-control study aimed to assess the efficacy of gray-scale ultrasonography and elastography in the prediction of HP. Aligning with Jeffery et al.'s results, our results showed that epigastric pain and loss of appetite were more common clinical manifestations in patients with HP infections ($p=0.022$ and 0.026, respectively).

Our results indicated that patients with positive HP infections had more AWT and MLT than gastritis patients with negative HP infections and that both have thicker AWT and MLT than those of normal individuals ($p<0.001$). These findings are consistent with a study by Pickhardt et al., who identified prominent circumferential 1.5–2 cm antral wall thickening as the most common manifestation of HP gastritis [16]. Another study determined that antral wall thickening is mostly due to physiological or benign causes, such as HP gastritis [17]. (Figs. 9, 10, 11 and 12) shows measurements of B-mode and elastography in several cases.

Confirming our results, Ergin et al. found that the most important cause of gastric wall thickening after tumors is chronic HP gastritis, which most frequently affects the gastric antrum. Furthermore, they observed that the antral wall reduced to normal thickness after HP eradication [18]. Another study by Kul et al. established that subclinical HP infection has no significant effect on gastric wall thickness [19].

Our measurements of AWT, MLT, and the MLT/AWT ratio were comparable to those of a previous study by Zaher et al., which reported 5.65±0.58, 3.02±0.43, and 0.53±0.04 measurements of AWT, MLT, and the MLT/AWT ratio, respectively, in patients with HP. They reported 4.57±0.82, 2.07±0.41, and 0.45±0.02 measurements of the AWT, MLT, and the MLT/AWT ratio, respectively, in patients with non-HP. They reported 3.93±0.52, 1.49±0.2, and 0.37±0.03 AWT, MLT, and the MLT/AWT ratio measurements, respectively, in the control group [8]. This strong similarity confirmed our study results and indicated that our findings can be implemented in the diagnostic medical imaging of gastritis.

Our study found that the strain ratio was significantly higher in + HP related to – HP and control group, consistent to our results Akbulut et al. mention that the strain

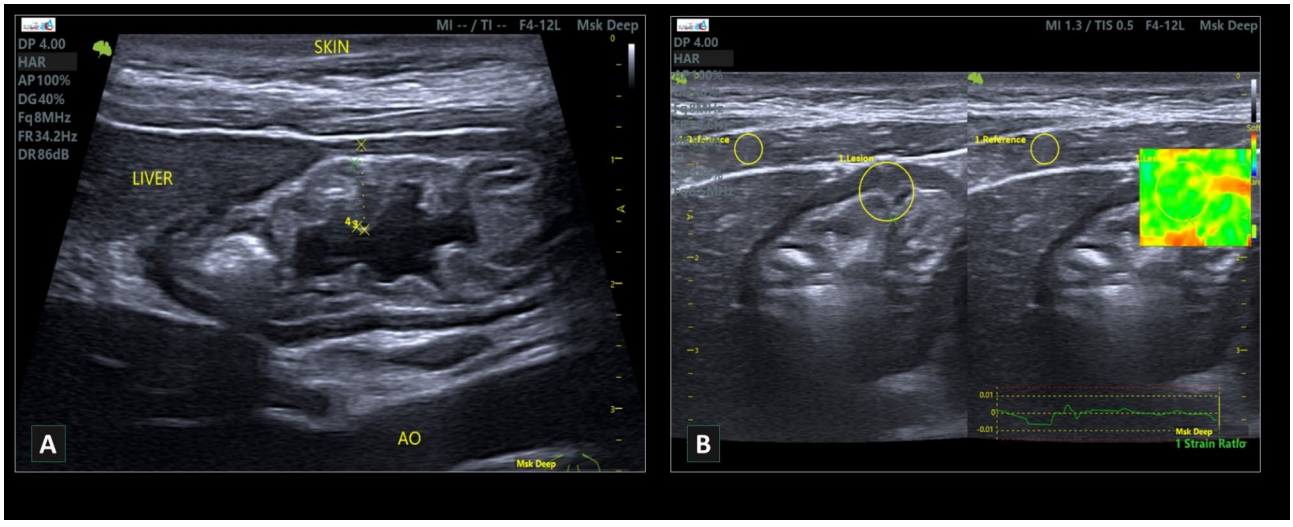

Fig. 9 B – mode and elastogram shows abnormal antral gastric wall measurements for 63 – years - male symptomized patient with positive of H. pylori infection presented with dysphagia, epigastric pain, and vomiting. Whereas AWT, MLT and MLT/AWT (6.83, 3.98 and 0.58 mm. respectively) and Strain Ratio 3.25

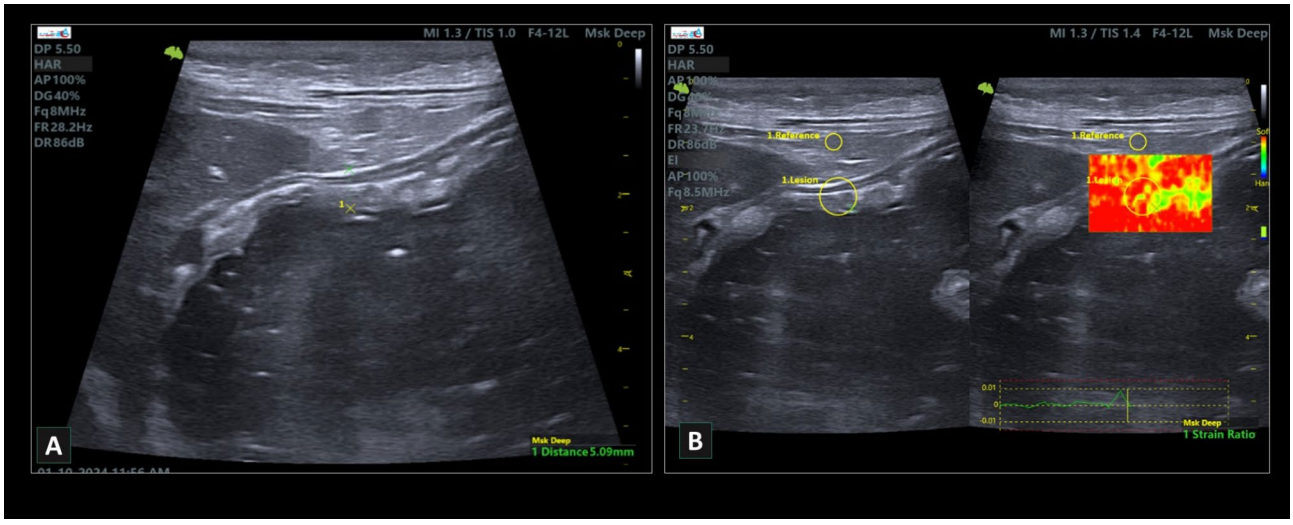

Fig. 10 B – mode and elastogram shows abnormal antral gastric wall measurements for 34- years - female symptomized patient conformed of HP

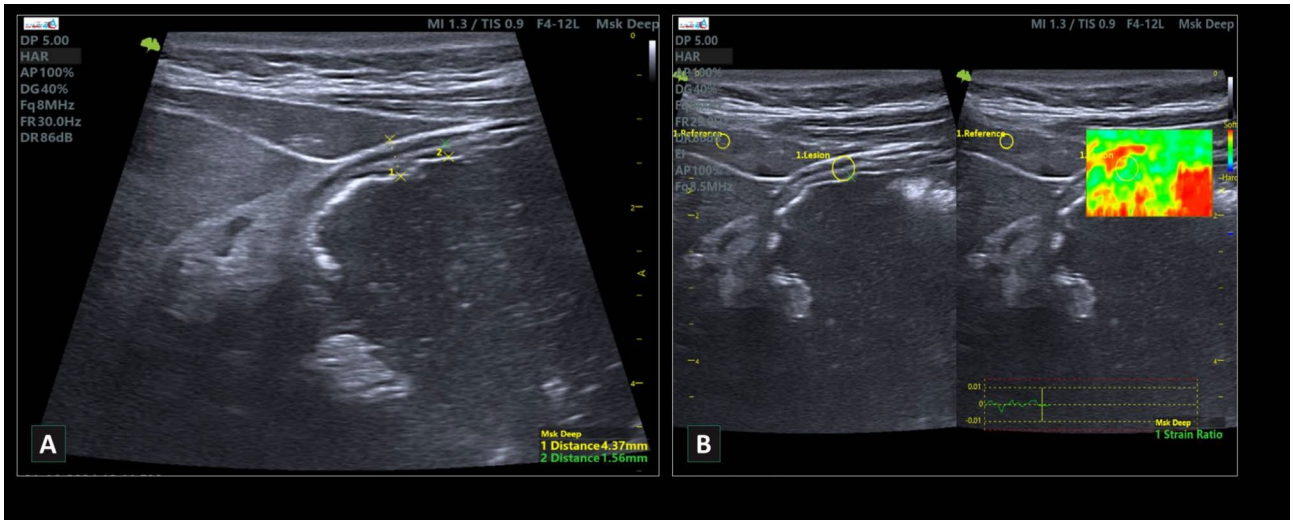

Fig. 11 B – mode and elastogram shows abnormal antral gastric wall measurements for 63 – years - male symptomized patient conformed of non - H. pylori infection through stool antigen screening presented with Epigastric pain, whereas AWT, MLT and MLT/AWT (4.37, 1.56 and 0.35 mm. respectively) and Strain Ratio 2.02

index values were more in gastritis positive pediatrics than in both negative gastritis and control group [2].

The current study results found that gray-scale ultrasonography is a highly effective imaging modality for HP prediction. These results substantiate the results of a previous study by Yazar et al. that identified transabdominal ultrasonography as an effective imaging modality for visualizing gastric antrum wall thickness and comfortably making gastritis diagnoses from gastric wall thickening measurements [20]. Our study found that B-mode ultrasonography achieved a sensitivity of 93.4%, while elastography achieved 95.1%, and that these values were elevated by using a combined evaluation (98.4%) for identifying patients with symptomatic HP among normal subjective groups. The current study confirms the findings of similar studies in different regions [2, 8], indicating that elastography is a promising imaging modality for diagnosing HP by measuring the AWT, MLT, and MLT/AWT ratio with the offer of a safely, radiation-free, and non-invasive method.

HP plays a causative role in gastritis, peptic ulcers, and gastric cancer. It also plays a role in extra-gastric diseases, such as metabolic syndrome, and hematologic disorders, such as vitamin B12, iron deficiency anemia, and cardiovascular disorders [21, 22]. The association between HP infection and nonalcoholic fatty liver disease is still controversial [23]. The effects of HP infection and the methods of diagnosing it are recommended topics for future studies.

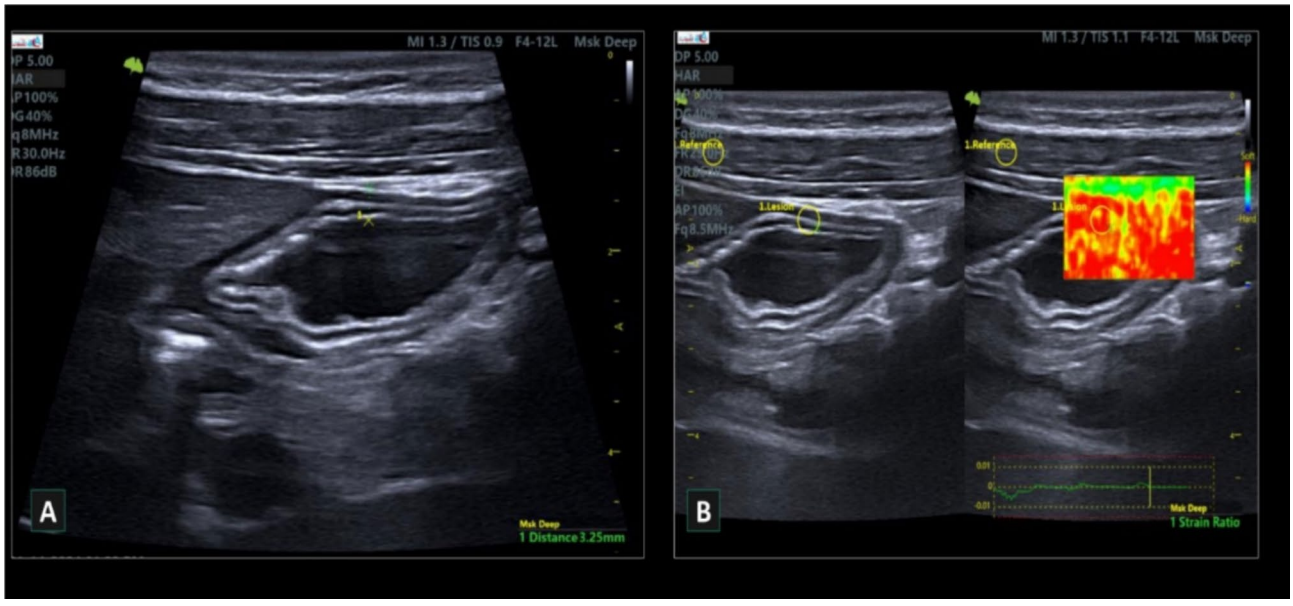

Fig. 12 B – mode and elastogram shows normal antral gastric wall measurements for 34 - years - female a symptomized patient conformed of negative H. pylori infection through stool antigen screening, whereas AWT, MLT and MLT/AWT (3.25, 1.32 and 0.40 mm. respectively) and Strain Ratio 1.4

The study faced some limitation insufficient long-term follow-up data on the potential of ultrasound and elastography for diagnosing HP. Furthermore, the final diagnosis of Heliobacter pylori on this study relied on noninvasive HP fecal antigen test or stool antigen test (SAT) results with lack of the gold standard gastric histopathology diagnosis, future research to compare the diagnostic accuracy of both fecal antigen testing and gastric biopsy as reference standards in estimating the diagnostic accuracy of B-Mode ultrasound and elastography could offer valued insights.

Conclusions

B-mode ultrasonography and elastography exhibit high discriminatory power in distinguishing symptomatic HP patients from normal individuals and differentiating (+) HP from negative HP, with greater discriminatory power when combined both imaging modalities.

Acknowledgements
The author extends their knowledge to Dr. Ahmed Alzomor Specialized Hospital (IBB City, Yemen) and the Alamel Specialized Hospital (Badan Locality–IBB, Yemen) for granting the approval for data collection in this study and helping us in data collection.

Author contributions
"Conceptualization, A.H. and A.G, MA; methodology, A.H.,A.G, A.M.A; software, A.H.,A.G; val-idation, A.A., A.G. and A.M.A., M.E.; formal analysis, R.A.A., M.G. K.A.; investigation, A.H.; resources, M.G, F.A.E, M.E.W.W.A, M.A.; data curation, AG, S.A.A; writing—original draft prepa-ration, S.A.A, A.G, A.H.; writing—review and editing, W.M.A, R.A.A, M.G; visualization, F.A.E., F.H.A and W.M.A. and R.A.A; supervision, M.E.,K.A, F.A.E; project administration, All authors.; funding acquisition, All authors have read and agreed to the published version of the manuscript.

Funding
This research received no external funding.

Data availability
Data are available from the first (corresponding author) upon reasonable request.

Declarations

Ethical approval and consent to participate
This study was approved by the Research Ethics Committee of the University of Medical Science and Technology (UMST), Graduate College, Sudan (No: UMST-FRS 0024/002), then approval was obtained from the area of the study. All procedures were conducted in conformity with the Declaration of Helsinki and all applicable standards and laws. Informed consent was obtained from all subjects involved in the study.

Consent for publication
Written informed consent has been obtained from the patient(s) to publish this paper.

Competing interests
The authors declare no competing interests.

Conflict of interest
The authors declare no conflicts of interest.

Author details
[1]Graduate College, University of Medical Science and Technology (UMST), Khartoum, Sudan
[2]Ultrasound Unit and Laboratory Department, Dr. Ahmed Alzomor Specialized Poly Clinic, Ibb 04-427015, Yemen
[3]Department of Diagnostic Radiology, College of Applied Medical Sciences, Taibah University, Al- Madinah Al-Munawwarah, Saudi Arabia
[4]Faculty of Medicine and Health Sciences, Department of Diagnostic Radiologic Technology, University of Science and Technology, Sana'a, Yemen
[5]Department of Radiological Sciences, College of Applied Medical Sciences, King Khalid University, Abha, Asir, Saudi Arabia

Received: 16 March 2024 / Accepted: 21 November 2024
Published online: 28 November 2024

References

1. Chey WD, Leontiadis GI, Howden CW, Moss SF. ACG clinical guideline: treatment of *Helicobacter pylori* infection. Am J Gastroenterol. 2017;112:212–39. https://doi.org/10.1038/ajg.2016.563.
2. Akbulut UE, Isik IA, Atalay A, Özkan MB. The usefulness of transabdominal ultrasound elastography in *Helicobacter pylori* gastritis in children. J Ultrasonography. 2023;23:61–5. https://doi.org/10.15557/jou.2023.0012.
3. Wang Y-K. Diagnosis of *Helicobacter pylori* infection: current options and developments. World J Gastroenterol. 2015;21:11221. https://doi.org/10.3748/wjg.v21.i40.11221.
4. Cardos AI, Maghiar A, Zaha DC, Pop O, Fritea L, Miere F, Cavalu S. Evolution of diagnostic methods for Helicobacter pylori infections: from traditional tests to high technology, advanced sensitivity and discrimination tools. Diagnostics. 2022;12:508. https://doi.org/10.3390/diagnostics12020508
5. Jones NL, Koletzko S, Goodman K, Bontems P, Cadranel S, Casswall T, Czinn S, Gold BD, Guarner J, Elitsur Y, et al. Joint ESPGHAN/NASPGHAN guidelines for the management of Helicobacter pylori in Children and adolescents (Update 2016). J Pediatr Gastroenterol Nutr. 2017;64:991–1003. https://doi.org/10.1097/mpg.0000000000001594.
6. Umegaki E, Misawa H, Handa O, Matsumoto H, Shiotani A. Linked color imaging for stomach. Diagnostics. 2023;13:467. https://doi.org/10.3390/diagnostics13030467.
7. Swenson DW, Wallach M. Helicobacter pylori–associated antral gastritis and ulcer disease. Ultrasound Q. 2012;28:185–7. https://doi.org/10.1097/ruq.0b013e318262cb5f.
8. Zaher T, Refaey M, Dawod H, Abo Warda M, Elfeky M, Amer S. The assessment of gastric antral wall thickness in Helicobacter pylori gastritis by abdominal ultrasonography, case-control study (2016–2018). Afro-Egyptian J Infect Endemic Dis. 2020;0:102–11. https://doi.org/10.21608/aeji.2020.25307.1055.
9. Alsaedi HI, Krsoom AM, Alshoabi SA, Alsharif WM. Investigation study of ultrasound practitioners' awareness about artefacts of hepatobiliary imaging in Almadinah Almunawwarah. Pakistan J Med Sci. 2022;38. https://doi.org/10.12669/pjms.38.6.5084.
10. Sun B, Liu J, Li S, Lovell JF, Zhang Y. Imaging of gastrointestinal tract ailments. J Imaging. 2023;9:115. https://doi.org/10.3390/jimaging9060115.
11. Branchi F, Caprioli F, Orlando S, Conte D, Fraquelli M. Non-invasive evaluation of intestinal disorders: the role of elastographic techniques. World J Gastroenterol. 2017;23:2832. https://doi.org/10.3748/wjg.v23.i16.2832.
12. Jiang Z, Nong B, Liang L, Yan Y, Zhang G. Differential diagnosis of Helicobacter pylori-associated gastritis with the linked-color imaging score. Dig Liver Disease. 2019;51:1665–70. https://doi.org/10.1016/j.dld.2019.06.024.
13. Salama NR, Hartung ML, Müller A. Life in the human stomach: persistence strategies of the bacterial pathogen Helicobacter pylori. Nat Rev Microbiol. 2013;11:385–99. https://doi.org/10.1038/nrmicro3016.
14. Jeffery PL. Endocrine impact of Helicobacter pylori: focus on ghrelin and ghrelin o-acyltransferase. World J Gastroenterol. 2011;17:1249. https://doi.org/10.3748/wjg.v17.i10.1249.
15. Cheung CK, Wu JC-Y. Role of Ghrelin in the pathophysiology of gastrointestinal disease. Gut Liver. 2013;7:505–12. https://doi.org/10.5009/gnl.2013.7.5.505.
16. Pickhardt PJ, Asher DB. Wall Thickening of the gastric Antrum as a normal finding:Multidetector CT with cadaveric comparison. Am J Roentgenol. 2003;181:973–9. https://doi.org/10.2214/ajr.181.4.1810973.
17. Akbas A, Bakir H, Dasiran MF, Dagmura H, Ozmen Z, Yildiz Celtek N, Daldal E, Demir O, Kefeli A, Okan I. Significance of gastric wall thickening detected in abdominal CT scan to predict gastric malignancy. J Oncol. 2019;2019:1–6. https://doi.org/10.1155/2019/8581547.
18. Ergin A, Çiyiltepe H, Karip AB, Fersahoğlu MM, Bulut NE, Çakmak A, Topaloğlu B, Bilgili AC, Somay A, Taşdelen İ, et al. The effect of Helicobacter pylori eradication on gastric wall thickness in patients undergoing laparoscopic sleeve gastrectomy. Obes Surg. 2021;31:4024–32. https://doi.org/10.1007/s11695-021-05513-8.
19. Kul S, Sert B, Sari A, Arslan M, Koşucu P, Ahmetoğlu A, Dinç H. Ffect of subclinical Helicobacter pylori infection on gastric wall thickness: multislice CT evaluation. Diagn Interv Radiol. 2008;14:138–42.
20. Yazar FM, Baykara M, Karaağaç M, Bülbüloğlu E. The role of conventional ultrasonography in the evaluation of antrum wall thickness in obese patients. Obes Surg. 2016;26:2995–3000. https://doi.org/10.1007/s11695-016-2221-1.
21. Han YM, Lee J, Choi JM, Kwak M-S, Yang JI, Chung SJ, Yim JY, Chung GE. The association between Helicobacter pylori with nonalcoholic fatty liver disease assessed by controlled attenuation parameter and other metabolic factors. PLoS ONE. 2021;16:e0260994. https://doi.org/10.1371/journal.pone.0260994.
22. Gravina AG, Priadko K, Ciamarra P, Granata L, Facchiano A, Miranda A, Dallio M, Federico A, Romano M. Extra-gastric manifestations of Helicobacter pylori Infection. J Clin Med. 2020;9:3887. https://doi.org/10.3390/jcm9123887.
23. Okushin K, Tsutsumi T, Ikeuchi K, Kado A, Enooku K, Fujinaga H, Moriya K, Yotsuyanagi H, Koike K. Helicobacter pyloriinfection and liver diseases: epidemiology and insights into pathogenesis. World J Gastroenterol. 2018;24:3617–25. https://doi.org/10.3748/wjg.v24.i32.3617.

Publisher's note